CHEMICAL ENGINEERING TRANSACTIONS

VOL. 41, 2014

A publication of AIDIC
The Italian Association of Chemical Engineering
www.aidic.it/cet

Guest Editors: Simonetta Palmas, Michele Mascia, Annalisa Vacca

ISBN 978-88-95608-32-7; **ISSN** 2283-9216

DOI: 10.3303/CET1441065

MoS_2/MoO_2/Graphene Electrocatalyst for HER

Maria Sarno*, Anna Garamella, Claudia Cirillo, Paolo Ciambelli

Department of Industrial Engineering and Centre NANO_MATES, University of Salerno
Via Giovanni Paolo II ,132 - 84084 Fisciano (SA), Italy
*Corresponding author: msarno@unisa.it

MoS_2 nanosheets have been successfully synthesized, on few layer graphene (FLG) obtained by physical exfoliation of graphite, by thermolysis of $(NH_4)_2MoS_4$, in a continuous flow reactor. The syntheses have been monitored with a mass spectrometer. After the precursor decomposition, an annealing treatment in N_2 to improve MoS_2 order, and in few percent of O_2 in N_2 to promote also MoO_2 nanocrystals formation, permits to obtain MoS_2/FLG and MoS_2/MoO_2/FLG hybrid materials via a solvent free, easily controllable and scalable process. The samples were characterized by Raman Spectroscopy, Electron Microscopy, and X-ray diffraction, and tested for HER activity using a typical three-electrode setup. We obtained excellent HER activity, with a Tafel slope compatible with electrochemical desorption as rate limiting step, while the presence of MoO_2 leads to a very low starting cathodic voltage of about 50 mV.

1. Introduction

Hydrogen is being vigorously pursued as future energy carrier and its sustainable production from water splitting is attracting growing attention. An advanced catalyst for the hydrogen evolution reaction (HER) should reduce the overpotential and consequently increase the efficiency of this important electrochemical process (Ramakrishna Matte et al., 2010). The most effective HER electrocatalysts are Pt-group metals, but it remains challenging to look for alternative catalysts based on materials that are more abundant at lower cost. Recent papers, (Jaramillo et al., 2007) reported excellent electrocatalytic activity for MoS_2 nanocatalyst (50-60 mV/dec), linearly dependent by the number of edge sites. The same authors (Bonde et al., 2008) prepared later a more commercially relevant nanocatalyst, MoS_2 nanoparticles on a Toray carbon paper, finding higher tafel slope (120 mV/dec) and exchange current density. MoS_2 nanoparticles supported on reduced graphene oxide (RGO) have shown excellent HER activity (Tafel slope of 41 mV/dec) with small overpotential (about 100 mV) (Li et al., 2011). Research efforts are addressed toward the synthesis of nanosized MoO_2 electrochemical materials through different routes (Zhao et al., 2013). Following the experiments on Ni-Mo based composites that have shown enhanced catalytic properties (Kubisztal et al., 2007), MoO_2 has been tested in combination with Ni for HER (Lacnjevac et al. 2012). Ni-MoO_2 possessed an order of magnitude higher intrinsic activity for HER in comparison with that of a flat Ni electrode. Very recently, an enhanced and stable electrocatalytic HER activity has been reported for MoO_2 nanobelts@nitrogen self-doped MoS_2 nanosheets (Zhou et al., 2014) (onset −156 mV (vs RHE), 105 mV more positive than that of pure MoS_2, and a Tafel slope of 47.5 mV/dec compared to a Tafel slope of 77.7 mV/dec for MoS_2, under identical experimental conditions), accounting for nitrogen doping that leads to enhanced electronic conductivity of the heterostructures as well as a high density of spinning electron states around the N and Mo atoms in MoS_2 nanosheets that are the active sites for HER. On the other hand, Chen et al. (Chen et al., 2011), to circumvent the conductivity limitation of MoS_2, combined it with a conductive MoO_3, obtaining high catalytic activity and stability. However, MoO_2 is more conductive than MoO_3, furthermore MoS_2 and MoO_2 nanostructures have never been used in combination with highly conductive graphene for HER. Here we report, the synthesis of MoS_2 nanosheets/few layer graphene (FLG) and of MoS_2/MoO_2/FLG hybrids by thermolysis of $(NH_4)_2MoS_4$, in a continuous flow reactor. FLG was obtained by physical exfoliation of graphite (Hernandez et al., 2008). After the precursor decomposition, an annealing treatment to improve MoS_2 order, and promote MoO_2 formation, was performed. In particular, the syntheses were monitored with a mass spectrometer to follow the evolution of

Please cite this article as: Sarno M., Garamella A., Cirillo C., Ciambelli P., 2014, Mos2/moo2/graphene electrocatalyst for her, Chemical Engineering Transactions, 41, 385-390 DOI: 10.3303/CET1441065

the reactions. This approach permits to obtain thin nanosheets of MoS_2, with also low lateral dimension exhibiting a large number of edges sites, together with small MoO_2 nanocrystals on graphene, via a solvent free, easily controllable and scalable process. The samples were characterized by Raman Spectroscopy, Electron Microscopy, Thermogravimetric analysis, X-ray diffraction, and tested for HER activity using a typical three-electrode setup.

2. Experimental

MoS_2 nanosheets has been prepared by thermolysis of ammonium thiomolybdates $(NH_4)_2MoS_4$ (Sigma Aldrich, purity of 99.99%) in N_2 environment (200 cm^3(STP)/min) and in presence of few layer graphene (FLG), thought two steps of conversion: (i) from room temperature to 400 °C + isotherm for 60 min; followed by (ii) a cooling form 400 °C to room temperature; and finally (iii) a step from room temperature to 1100 °C + isotherm (in N_2 for 30 min) sample **S1**, (in N_2 for 30 min followed by 45 min in 0.2 vol.% of O_2 in N_2) sample **S2**. FLG were obtained by a sonication of graphite in N-methylpyrrolidone (NMP, spectrophotometric grade> 99.0%) at a concentration of 10 mg/ml for 1 h at the maximum power of ultrasound (Hielscher UP 400S). FLG were recovered by vacuum filtration of the supernatant solution after a centrifugation (the supernatant contains about the 30 wt% of the original graphite - TG evaluation, not reported here), onto: porous alumina membranes (pore size: 20 nm). Before the synthesis, $(NH_4)_2MoS_4$ and FLG (50 wt.% for each component) were sonicated in water for 30 min, after drying at 130 °C, the powder mixture was loaded in a continuous flow microreactor, consisting in a quartz tube (16 mm internal diameter, 300 mm length) (Altavilla et al., 2011; Altavilla et al., 2013; Ciambelli et al., 2011; Giubileo et al., 2012; Sarno et al., 2012; Sarno et al., 2013a; Sarno et al., 2013b). All the samples obtained were characterized by the combined use of different techniques. Transmission electron microscopy (TEM) images were acquired using a FEI Tecnai electron microscope operated at 200 KV with a LaB6 filament as the source of electrons, equipped with an EDX probe. Scanning electron microscopy (SEM) images were obtained with a LEO 1525 microscope. Raman spectra were obtained at room temperature with a micro-Raman spectrometer Renishaw inVia with a 514 nm excitation wavelength (laser power 30 mW) in the range 100-3000 cm^{-1}. Optical images were collected with a Leica DMLM optical microscope connected on-line with the Raman instrument. For all the sample about 40 measurements have been carried out. The laser spot diameter was about 10 µm. XRD measurements were performed with a Bruker D8 X-ray diffractometer using CuK_α radiation. Thermogravimetric analysis (TG-DTG) at a 10 K/min heating rate in flowing air was performed with a SDTQ 600 Analyzer (TA Instruments) coupled with a mass spectrometer. For the electrochemical measurements 4 mg of catalyst were dispersed in 80 µl of 5 wt% Nafion solution to form a homogeneous ink. Then the catalyst ink was loaded onto a glassy carbon electrode of 3 mm in diameter. Linear sweep voltammetry (using the pontentiostat from Amel Instruments) with scan rate of 2 mVs^{-1} was conducted in 0.5 M H_2SO_4, using saturated calomel electrode as the reference electrode, a graphite electrode as the counter electrode and a loadable glassy carbon electrode as the working electrode.

3. Results and discussion

The thermolysis of ammonium thiomolybdates $(NH_4)_2MoS_4$ has been extensively studied (Berntsen et al., 2008). It has been reported that $(NH_4)_2MoS_4$ thermolysis in an N_2 environment resulted in the conversion of $(NH_4)_2MoS_4$ to MoS_3, releasing ammonia and hydrogen sulfide to the gas phase ($(NH_4)_2MoS_4 \rightarrow 2NH_3 + H_2S + MoS_3$) at lower temperatures, followed by a conversion of MoS_3 to highly disordered MoS_2 ($MoS_3 \rightarrow MoS_2 + S$), the product remained amorphous up to around 350 °C, while crystallinity set in at 400 °C when first vague lines appeared on the diffractograph. To improve the MoS_2 quality, it is rational to increase the thermolysis temperature. Although a measure of agreement is evident in the previous studies, there is ambiguity in the transition temperatures, nor nanostructures synthesis studies in presence of graphene have been performed. We develop the syntheses in two steps, the first one between 25-400 °C, to obtain disordered MoS_2 on FLG, further annealed for 60 min, the second step between 25 to 1100 °C, followed by 30 or 75 min (see experimental section for details) to further improve the degree of order and promote the formation of MoO_2. In particular, in Figure 1a the thermogravimetric (TG-DTG) and temperature profiles, during the test simulating the **S1** synthesis conditions, are reported as function of time. It is possible to distinguish five temporal phases: (I) from room temperature to 400 °C; (II) 1h in isotherm at 400 °C; (III) from 400 °C to room temperature (not followed by the thermobalance); (IV) from room temperature to 1100 °C; (V) 30 min in isotherm at 1100 °C. After an initial weight loss due to water (22.3 wt.%), the DTG profile shows a sharp weight loss due to NH_3 and H_2S release, as clearly indicated by the corresponding total ion current (TIC) of the most intense mass fragments peaks: m/z = 15, 16, 17 form

NH_3 and 32, 33, 34 from H_2S (reaction 1). The NH_3 and H_2S release completing at about 360 °C. At 170 °C a sulphur release starts, with a maximum at about 380 °C, compatible with the evolution of reaction 2. A further 3 wt.% is lost in the 60 min isothermal step at 400 °C. During the further temperature increase (phase IV) and starting from 400 °C a further sulphur release (m/z=32) happens, the TG residue at 1100 °C (about 61 wt.%) being compatible with the starting amount of FLG and the formation of MoS_2 from the precursor. From sending oxygen, a weight loss is also registered during the high temperature isotherm, firstly due to MoS_2 and than to FLG oxidations, with SO_2 (m/z=64) and CO_2 (m/z=44) releases (see again Fig. 1a).

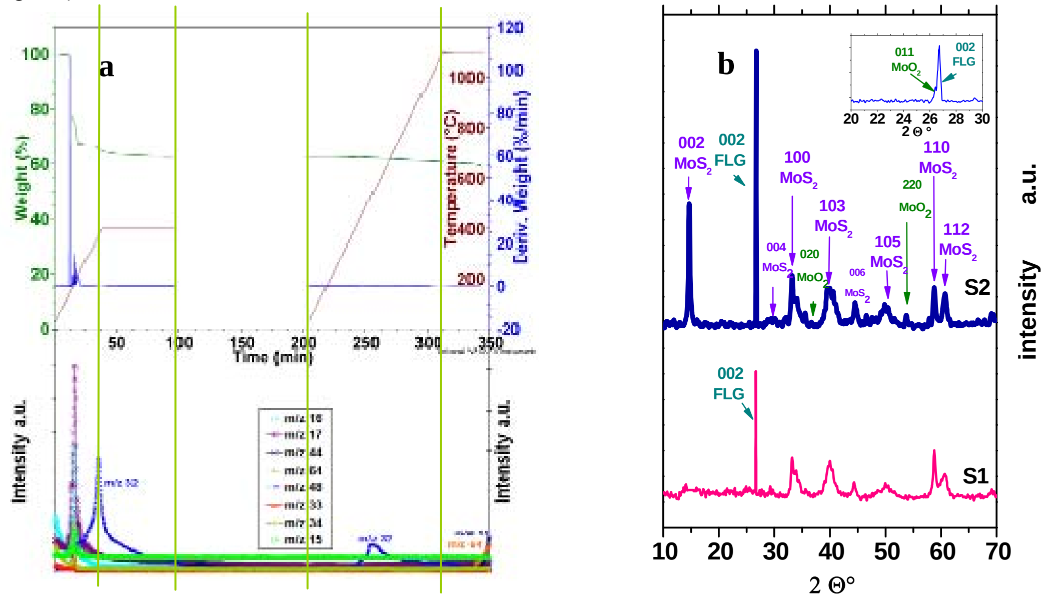

Figure 1. TG-DTG profiles, during the test simulating the S1 synthesis conditions, and the corresponding TIC (a). XRD diffraction patterns of the samples after the two steps of synthesis and for different annealing time at 1100 °C (b).

The XRD patterns recorded on the decomposition products after annealing at specific times are shown in Figure 1b. The sample after the first step of annealing exhibits the loss of the original precursor structure and the typical x-ray pattern of amorphous MoS_2 (Sarno et al., 2014b). After the second step of thermolysis the typical spectrum of 2H-MoS_2 is shown for both the samples, **S1** exhibits a very broad (002) reflection (Berntsen et al., 2008; Leist et al., 1998), while **S2** a more pronounced sawtooth (002) peak, indicating a progressive in-plane restacking, also the typical monoclinic MoO_2 peaks appear timidly, likely due to an oxidation phenomenon. In both the spectra the (002) reflection from FLG is clearly visible. FLG flakes have a lateral size of few micrometres. Most of the FLG sample consists of flakes with less than 6 sheets and a number fraction of monolayer graphene (number of monolayers/total number of flakes observed) in NMP dispersions of 22%. In the sample a fraction of flakes (about 6% total based) with a number of sheets between 30 and 40, are also present (Sarno et al., 2014a). Figure 2a shows a typical Raman spectrum of sample **S2** excited by 514 nm line in air ambient environment. A_{1g} and E'_{2g} modes for MoS_2 are clearly observed at about 382 and 407 cm^{-1}, respectively, together with less intense typical Raman bands of MoO_2 (200, 229, 355, 489 cm^{-1}), in the range 200-500 cm^{-1}. In the high wavelength range the typical spectrum of FLG is also reported. The two most intense features are the G peak at ~1570 cm^{-1} and the 2D band at ~2700 cm^{-1} (Casiraghi et al., 2005), which differs from that typical for graphite, consisting of two components $2D_1$ and $2D_2$ the second with an highest intensity than the first, has a quite flat apex and can be easily deconvolved with almost two peaks. A broad D-band can be also seen, likely due to the FLG edges (taking into account the laser spot dimension and the flakes size (Sarno et al., 2014a)). Similar to the case of graphene, Raman spectroscopy can be employed to characterize the thickness of MoS_2 nanolayers. As reported by Lee et al. (Lee et al., 2010), the frequency difference between the two most prominent Raman peaks depends monotonically on the number of MoS_2 layers. The results from these evaluation, performed on a number of significant Raman spectra for **S1** and **S2** are shown in Figure 2b. The sheets shown an increasing number of layers under annealing time increase, in any case lower than 13.

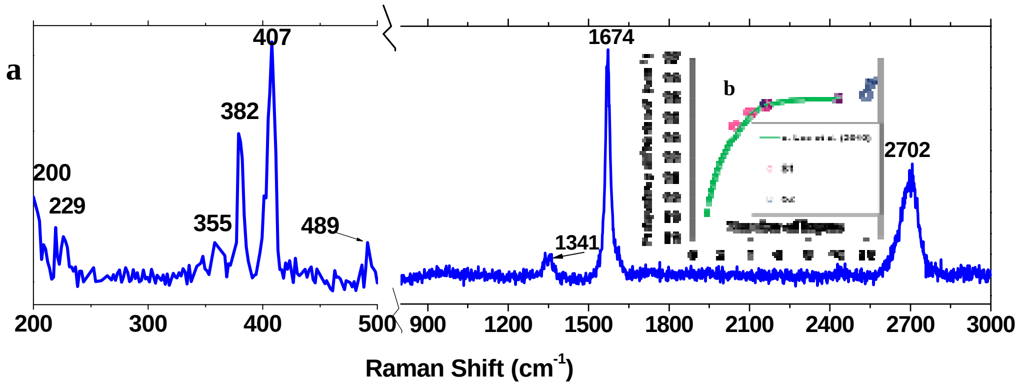

*Figure 2. Raman Spectra of **S2** in the range 200-3000 cm^{-1}(a) and the frequency difference between A_{1g} and E'_{2g} Raman modes (b).*

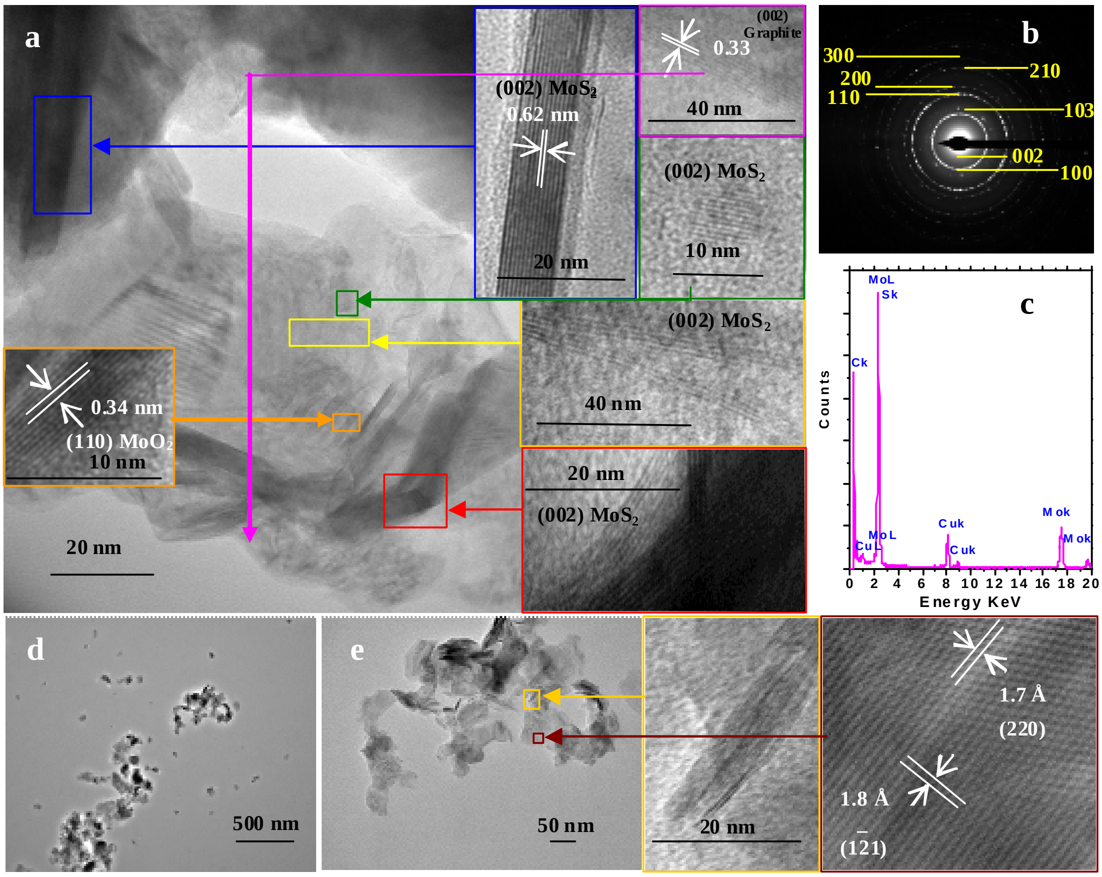

*Figure 3. **S2** TEM image (a), high resolution TEM images in the inserts. **S1** SAED pattern (b) and EDS spectrum (c). MoS_2/MoO_2 TEM images at different magnification (d,e), high resolution TEM images in the inserts.*

Figure 3a shows bright-field TEM images, at different magnifications of **S2**. MoS_2 nanosheets lay on FLG, with some folded edges exhibiting parallel lines corresponding to the different layers of MoS_2 (number of layers = 3-13), as evidenced by high resolution images in the inserts of Figure 3a. It is also possible to observe, on graphene, crystals, attributable to MoO_2 (see the insert showing periodic fringe spacing ~3.4 Å that agree well with the interplanar spacing between the {110} planes of monoclinic MoO_2) resulting from an oxidation of MoS_2 to form MoO_2. The TEM characterization reveals also the presence of FLG (see the insert showing the (002) interplanar spacing of 0.33 nm typical of graphite, from FLG support edge). FLG, that were obtained by a physical exfoliation of graphite (Sarno et al., 2014a), have: lateral sizes of few micrometres; a number fraction of monolayer graphene (number of monolayers/total number of flakes) is equal to 22%; and more than 85% of the total sheets number have layers ranging from 1 to 13. In Figure 3b and 3c, the selected area diffraction (SAED) pattern of MoS_2, and the energy dispersive TEM based X-ray spectroscopy (EDS) (confirming the S/Mo ratio ~ 2.at.), obtained under **S1** exploration, are shown, respectively. In Figure 3d and 3e two TEM images, at different magnification, of a sample obtained in the same operating conditions of **S2** but graphene, to better highlight the arrangement state of MoS_2 and MoO_2 nanocrystals, more difficult to assess in the presence of the additional graphene layer under electron beam, are shown. The nanocrystals have a size of few hundreds nanometers, in the sample MoS_2 nanosheets and MoO_2 nanoparticles, segregated and intimately connected, are visible (see the high resolution TEM images in the inserts of Figure 3e, where the typical MoS_2 parallel lines, and the periodic fringe spacing of ~1.7 Å and ~1.8 Å agree well with the interplanar spacing between the {220}, and $\{1\bar{2}1\}$ planes of monoclinic MoO_2, can be seen, respectively).

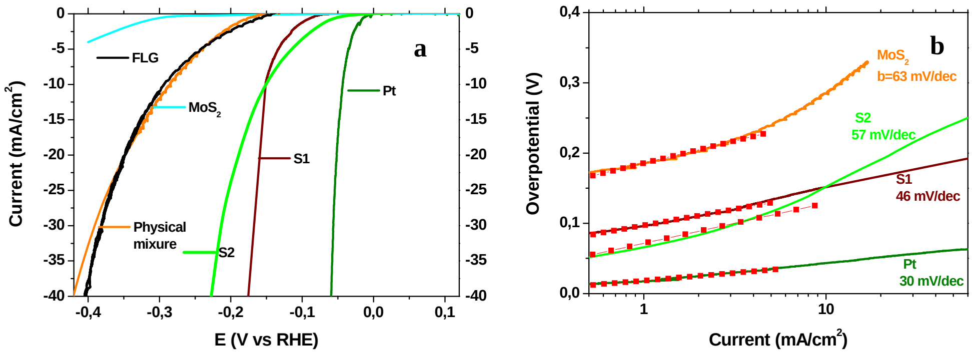

Figure 4. Polarization curves obtained with several catalysts deposited on glassy carbon electrodes (a), and corresponding Tafel plot (b).

We investigated the electrocatalytic HER activities of our hybrid materials deposited on a glassy carbon electrode in 0.5 M H_2SO_4 solutions using a typical three-electrode setup (Figure 4a). As a reference point, we also measured a commercial Pt catalyst with high HER catalytic performances. Polarization curve (i-V plot) recorded with **S1** showed a small overpotential of ~0.08 V for HER, beyond which the cathodic current rose rapidly under more negative potentials. In sharp contrast, free MoS_2 nanosheets or FLG alone exhibited little HER activity. MoS_2 nanosheets physically mixed with FLG at a similar C:Mo ratio also showed inferior performance to **S1**. Linear portions of the Tafel plots (Figure 4b) were fit to the Tafel equation ($\eta = b \log j + a$, where η is the overpotential, j is the current density, b is the Tafel slope), yielding Tafel slopes of ~30, ~46 and ~63 mV/decade (iR-corrected) for Pt, **S1** and free MoS_2 nanosheets, respectively. The observed Tafel slope suggests that electrochemical desorption is the rate limiting step (Li et al., 2011), the high performance likely due to an electronic coupling between the FLG and MoS_2 sheets. It is worth to notice, that even if **S2** shows an higher Tafel slope, it exhibits a very low onset of cathodic voltage. To better understand the basic reasons of this behaviour, probably due to a sort of electronic synergy between the various components and that could get to the development of a new even more efficient catalyst, further investigation are required.

4. Conclusions

MoS_2/FLG and MoS_2/MoO_2/FLG hybrids have synthesized via a solvent free, easily controllable and scalable process. The samples were wide characterized by the combined use of different techniques and tested for HER. MoS_2 nanosheets and MoO_2 nanoparticles lay on FLG. We obtained excellent HER activity due to an electronic coupling between FLG and the nanoparticles, with a Tafel slope compatible with electrochemical desorption as rate limiting step, while the presence of MoO_2 leads to a very low starting cathodic voltage of about 50 mV, deserving further investigation to develop an even more efficient electrode.

References

Altavilla C., Sarno M., Ciambelli P., 2011, A Novel Wet Chemistry Approach for the Synthesis of Hybrid 2D Free-Floating Single or Multilayer Nanosheets of MS_2@oleylamine (M=Mo, W), Chem. Mater. 23, 3879-3885.

Altavilla C., Sarno M., Ciambelli P., Senatore A., Petrone V., 2013, New 'chimie douce' approach to the synthesis of hybrid nanosheets of MoS_2 on CNT and their anti-friction and anti-wear properties, Nanotechnology 24, 125601 (11pp).

Berntsen N., Gutjahr T., Loeffler L., Gomm J. R., Seshadri R., Tremel W., 2008, A Solvothermal Route to High-Surface-Area Nanostructured MoS_2, Chem. Mater. 15, 4498-4502.

Bonde J., Moses P. G., Jaramillo T. F., Norskov J.K., Chorkendorff I., 2008, Hydrogen evolution on nano-particulate transition metal sulfides, Faraday Discuss. 140, 219-231.

Casiraghi C., Ferrari A.C., Robertson J., 2005, Raman spectroscopy of hydrogenated amorphous carbons, Phys. Rev. B 72, 085401 (14pp).

Chen Z., Cummins D., Reinecke B. N., Clark E., Sunkara M. K., Jaramillo T.F., 2011, Core–shell MoO_3-MoS_2 Nanowires for Hydrogen Evolution: A Functional Design for Electrocatalytic Materials, Nano Lett. 11, 4168-4175.

Ciambelli P., Arurault L., Sarno M., Fontorbes S., Leone C., Datas L., Sannino D., Du Plouy Sle B., 2011, Controlled growth of CNT in mesoporous AAO through optimized conditions for membrane preparation and CVD operation, Nanotechnology 22, 265613.

Giubileo F., Di Bartolomeo A., Sarno M., Altavilla C., Santandrea S., Ciambelli P., Cucolo A.M., 2012, Field emission properties of as-grown multiwalled carbon nanotube films, Carbon 50, 163-169.

Hernandez Y., Nicolosi V., Lotya M., Blighe F.M., Sun Z., De S., McGovern I.T., Holland B., Byrne M., Gun'ko Y.K., Boland J.J., Niraj P., Duesberg G., Krishnamurthy S., Goodhue R., Hutchison J., Scardaci V., Ferrari A.C., Coleman J.N., 2008, High-yield production of graphene by liquid-phase exfoliation of graphite, Nat. Nanotechnol. 3, 563-568.

Jaramillo T.F., Jørgensen K.P., Bonde J., Nielsen J.H., Horch S., Chorkendorff I., 2007, Identification of Active Edge Sites for Electrochemical H_2 Evolution from MoS_2 Nanocatalysts, Science 317, 100-102.

Kubisztal J., Budniok A., Lasia A., 2007, Study of the hydrogen evolution reaction on nickel-based composite coatings containing molybdenum powder, Int. J. Hydrogen Energy 32, 1211-1218.

Lacnjevac U.C., Jovic B.M., Jovic V.D., Krstajic N.V., 2012, Determination of kinetic parameters for the hydrogen evolution reaction on the electrodeposited Ni–MoO_2 composite coating in alkaline solution, J. Electroanal Chem 677-680, 31-40.

Lee C., Yan H., Bruns L. E., Heinz T. F., Hone J., Ryu S., 2010, Anomalous lattice vibrations of single- and few-layer MoS_2, ACS Nano 4, 2695-2700.

Leist A., Stauf S., Loken S., Finckh E. W., Ludtke S., Unger K.K., Assenmacher W., Mader W., Tremel W., 1998, Semiporous MoS_2 obtained by the decomposition of thiomolybdate precursors J. Mater. Chem. 8, 241-244.

Li Y., Wang H., Xie L., Liang Y., Hong G., Dai H., 2011, MoS_2 Nanoparticles Grown on Graphene: An Advanced Catalyst fort he Hydrogen Evolution Reaction, J. Am. Chem. Soc. 133, 7296-7299.

Ramakrishna Matte H.S.S., Gomathi A., Manna A.K., Late D.J., Datta R., Pati S.K., Rao C.N.R., 2010, MoS_2 and WS_2 Analogues of Graphene, Angew. Chem.122, 4153-4156.

Sarno M., Cirillo C., Piscitelli R., Ciambelli P., 2013a, A study of the key parameters, including the crucial role of H_2 for uniform graphene growth on Ni foil, J. Mol. Catal. A: Chem. 366, 303-314.

Sarno M., Garamella A., Cirillo C., Ciambelli P., 2014a, MoO_2 synthesis for LIBs, Chem. Eng. Trans., accepted.

Sarno M., Garamella A., Cirillo C., Ciambelli P., 2014b, MoS_2 nanosheets for HER and LIB, Chem. Eng.Trans., submitted.

Sarno M., Sannino D., Leone C., Ciambelli P., 2012, Evaluating the effects of operating conditions on the quantity, quality and catalyzed growth mechanisms of CNTs, J. Mol. Catal. A: Chem. 357, 26-38.

Sarno M., Tamburrano A., Arurault L., Fontorbes S., Pantani R., Datas L., Ciambelli P., Sarto M.S., 2013b, Electrical conductivity of carbon nanotubes grown inside a mesoporous anodic aluminium oxide membrane, Carbon 55, 10-22.

Zhao Y., Zhang Y., Yang Z., Yan Y., Sun K., 2013, Synthesis of MoS_2 and MoO_2 for their applications in H_2 generation and lithium ion batteries: a review, Sci. Technol. Adv. Mater. 14, 043501 (12pp).

Zhou W., Hou D., Sang Y., Yao S. H., Zhou J., Li G., Li L., Liu H., Chen S., 2014, MoO2 nanobelts@nitrogen self-doped MoS_2 nanosheets as effective electrocatalysts for hydrogen evolution reaction, J. Mater. Chem. A, Accepted.